US009304299B2

(12) **United States Patent**
Yin et al.

(10) **Patent No.: US 9,304,299 B2**
(45) **Date of Patent: Apr. 5, 2016**

(54) **FOUR-PIECE ALL-ASPHERIC ADAPTER FISHEYE LENS**

(71) Applicant: **OmniVision Technologies, Inc.**, Santa Clara, CA (US)

(72) Inventors: **Chuen-Yi Yin**, New Taipei (TW); **Jau-Jan Deng**, Taipei (TW)

(73) Assignee: **OmniVision Technologies, Inc.**, Santa Clara, CA (US)

(*) Notice: Subject to any disclaimer, the term of this patent is extended or adjusted under 35 U.S.C. 154(b) by 100 days.

(21) Appl. No.: **14/465,146**

(22) Filed: **Aug. 21, 2014**

(65) **Prior Publication Data**

US 2016/0054547 A1 Feb. 25, 2016

(51) **Int. Cl.**

G02B 3/02	(2006.01)
G02B 13/18	(2006.01)
G02B 9/12	(2006.01)
G02B 13/06	(2006.01)
G02B 9/34	(2006.01)
G02B 27/00	(2006.01)
G03B 17/56	(2006.01)

(52) **U.S. Cl.**

CPC ***G02B 13/06*** (2013.01); ***G02B 9/34*** (2013.01); ***G02B 13/18*** (2013.01); ***G02B 27/0025*** (2013.01); ***G03B 17/565*** (2013.01)

(58) **Field of Classification Search**

CPC G02B 13/004; G02B 9/34; G02B 13/04; G02B 13/18; G02B 13/0035; G02B 9/12; G02B 9/16; G03B 17/565; G03B 17/14

USPC 359/648, 672–675, 715, 716, 753, 781, 359/784

See application file for complete search history.

(56) **References Cited**

U.S. PATENT DOCUMENTS

3,734,600	A *	5/1973	Shimizu	G02B 13/06 359/723
6,128,145	A *	10/2000	Nagaoka	H04N 7/183 359/749
6,504,655	B2	1/2003	Shibayama	
7,023,628	B1 *	4/2006	Ning	G02B 13/06 359/680

(Continued)

OTHER PUBLICATIONS

Symmons, et al. "Molded Optics: Precision Molded Glass Challenges Plastic Optics," retrieved from http://www.laserfocasworld.com/articles/2011/07/molded-optics-precision-molded-glass-challenges-plastic-optics.html Jul. 1, 2011.

(Continued)

Primary Examiner — Evelyn A Lester

(74) *Attorney, Agent, or Firm* — Lathrop & Gage LLP

(57) **ABSTRACT**

A four-piece all-aspheric adapter fisheye lens includes a negative meniscus lens, a biconcave lens, a positive meniscus lens, and a biconvex lens. The biconcave lens is between the negative meniscus lens and the positive meniscus lens; the positive meniscus lens is between the biconcave lens and the biconvex lens. The negative meniscus lens, the biconcave lens, the positive meniscus lens, and the biconvex lens are coaxial and arranged with an exit pupil to cooperatively generate an image with a camera lens that has greater field of view than the camera lens alone when the exit pupil is coplanar and coaxial with an entrance pupil of the camera lens. Each of the negative meniscus lens, the biconcave lens, the positive meniscus lens, and the biconvex lens has an aspheric object-side surface and an aspheric image-side surface.

17 Claims, 14 Drawing Sheets

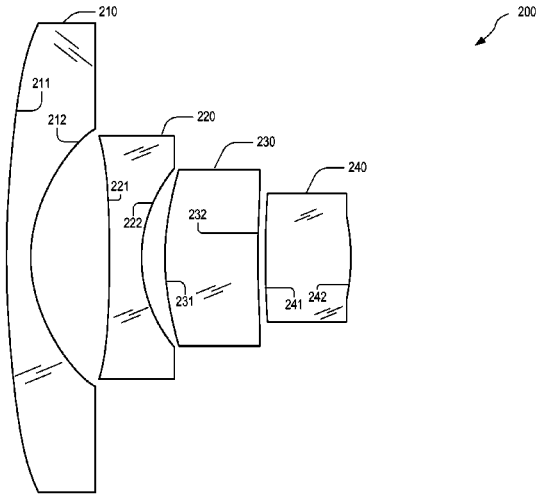

(56) **References Cited**

U.S. PATENT DOCUMENTS

8,134,787	B2 *	3/2012	Saitoh	G02B 13/06 359/715
8,279,544	B1	10/2012	O'Neill	
8,570,660	B2	10/2013	Takemoto et al.	
2006/0274433	A1 *	12/2006	Kamo	G02B 15/177 359/793
2007/0139793	A1 *	6/2007	Kawada	G02B 13/06 359/740
2008/0239517	A1 *	10/2008	Mori	G02B 9/34 359/781
2009/0080093	A1 *	3/2009	Ning	G02B 13/06 359/753
2010/0246029	A1 *	9/2010	Asami	G02B 13/004 359/708
2011/0085245	A1	4/2011	Kim	
2012/0113532	A1 *	5/2012	Lee	G02B 13/06 359/753
2014/0128673	A1	5/2014	Cheng	

OTHER PUBLICATIONS

Pontinen, "Study on Chromatic Aberration of Two Fisheye Lenses," The Intl Archives of Photogrammetry, Remote Sensing and Spatial Information Services, vol. XXXVII, Part B3a, Beijing 2008.

* cited by examiner

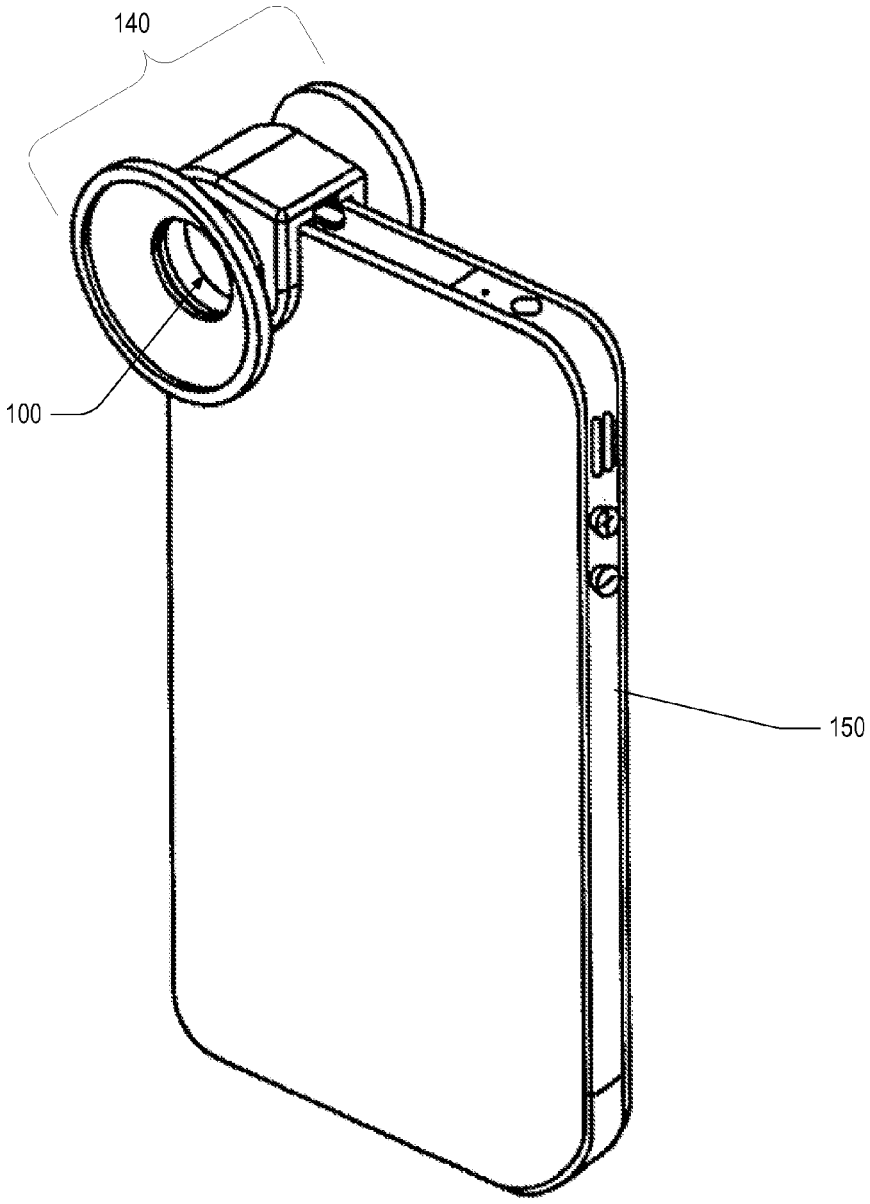

PRIOR ART

FIG. 1

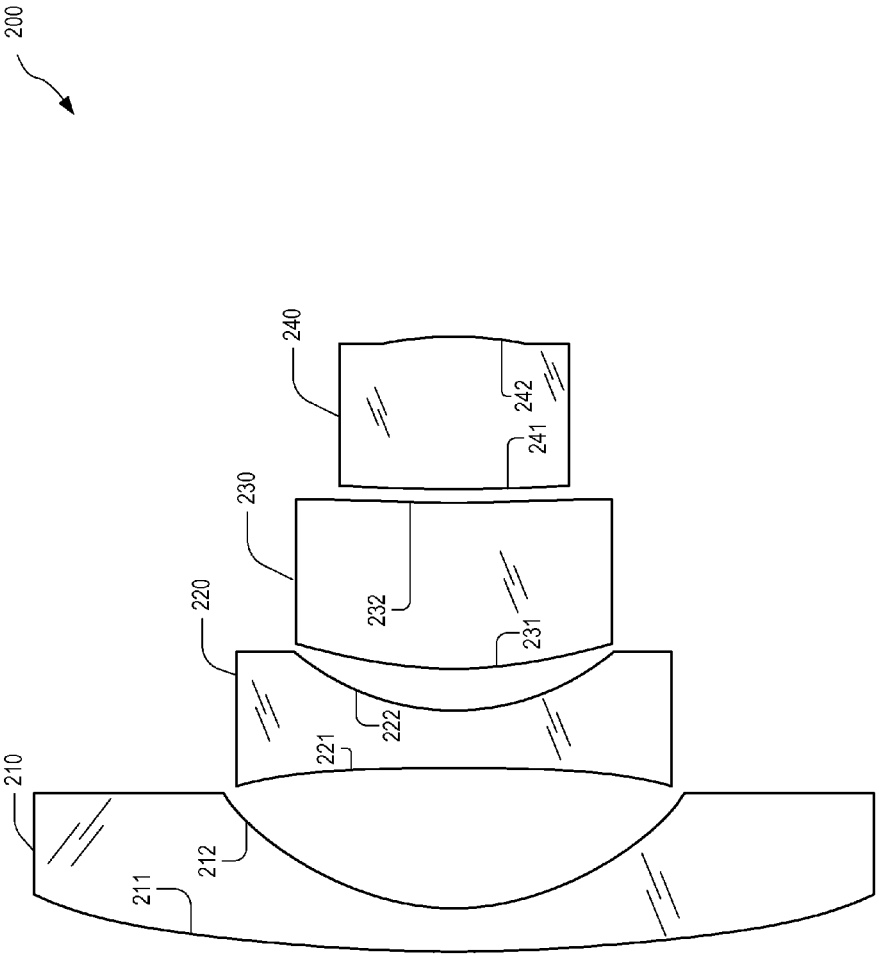

FIG. 2

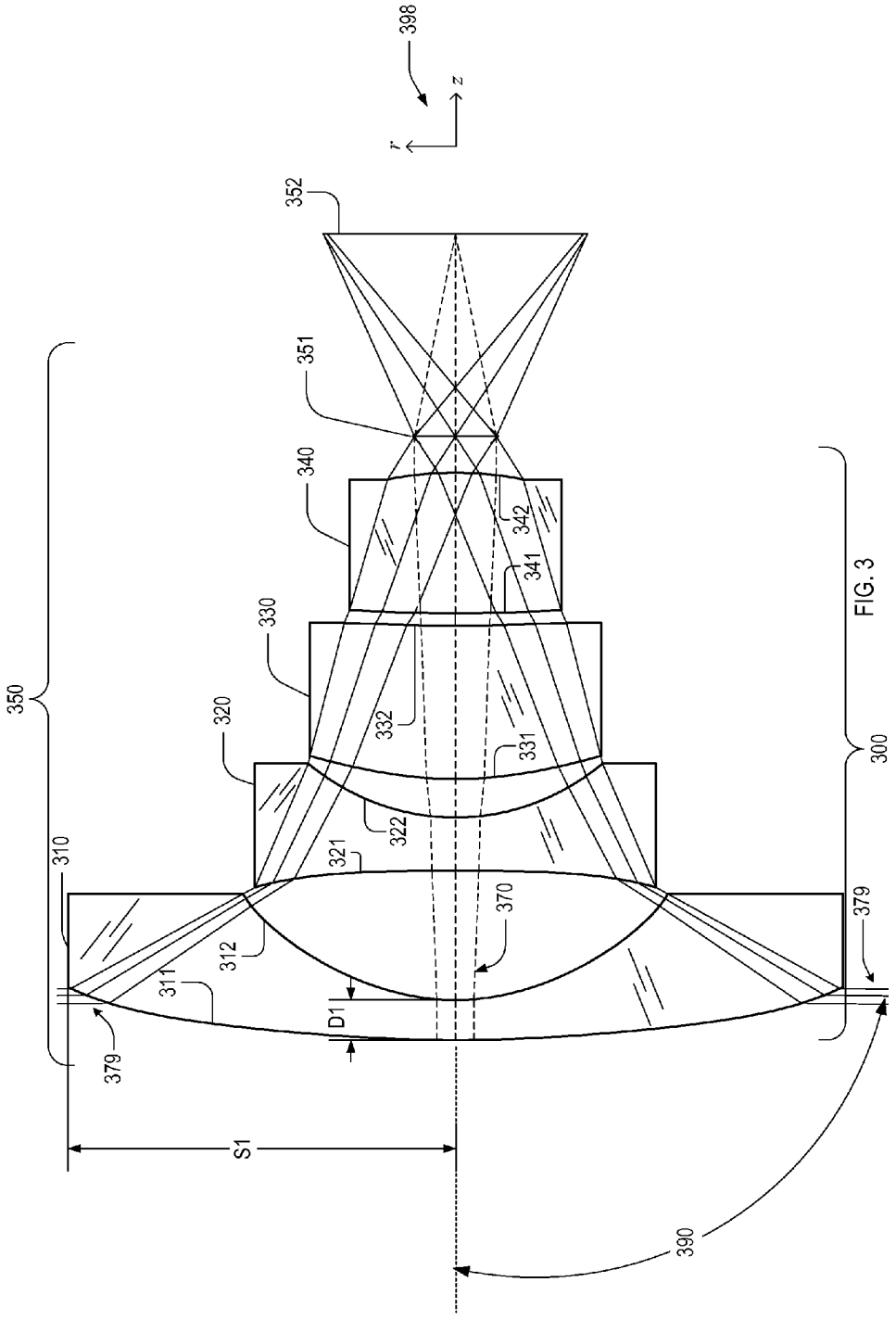
398
z
r
352
351
340
342
341
330
332
331
320
322
321
310
312
311
370
379
379
D1
S1
350
300
390

FIG. 3

411	412	413	414	415	416	404	406	408	410
	radius					aspheric coefficient			
surface	r_c (mm)	thickness (mm)	n_D (λ=589 nm)	Abbe Number	conic k	4th-order term α_4	6th-order term α_6	8th-order term α_8	10th-order term α_{10}
object	∞	∞	--	--	--	--	--	--	--
311	21.071	0.551	1.543	57	-0.053	-5.8015E-04	2.2653E-05	--	--
312	3.078	1.789			-0.013	-9.1296E-03	8.0853E-04	-8.3278E-05	--
321	-41.543	0.733	1.543	57	-176.992	-2.2302E-03	-6.2052E-05	--	--
322	3.126	0.532			-0.063	2.8471E-03	-8.3299E-04	6.8817E-05	--
331	5.386	2.114	1.632	23	-7.015	1.6435E-04	-7.8896E-06	0.0000E+00	--
332	16.782	0.174			-184.843	-2.4209E-03	-2.0615E-05	--	--
341	20.303	1.941	1.510	57	-197.957	-7.6131E-04	3.5204E-04	--	--
342	-4.746	0.500			11.308	5.7934E-03	2.3631E+06	-2.6596E-02	1.7262E-02
351	∞	2.800	(ideal lens)		--	--	--	--	--
352	∞	--	--	--	--	--	--	--	--

FIG. 4

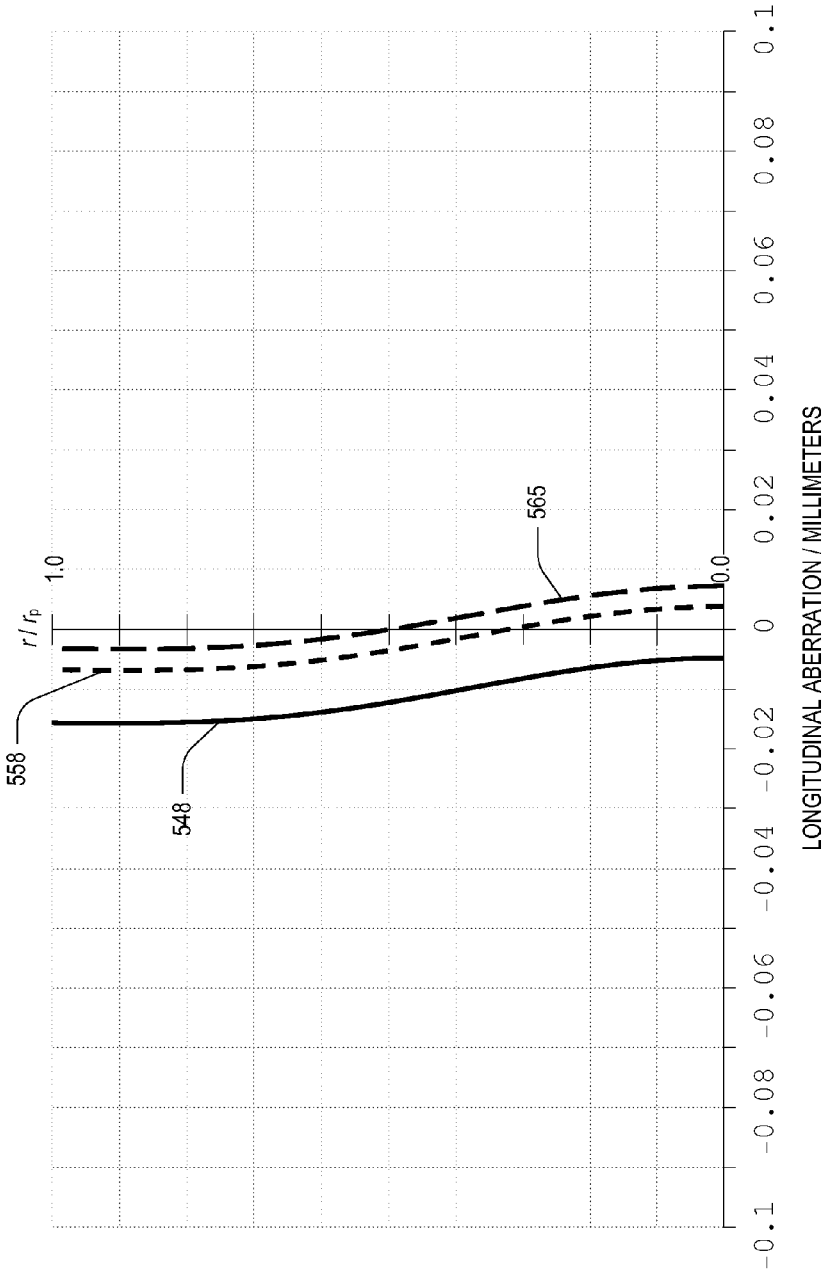
0.1
0.08
0.06
0.04
0.02
0
-0.02
-0.04
-0.06
-0.08
-0.1
LONGITUDINAL ABERRATION / MILLIMETERS
0.0
1.0
r / r_p
565
558
548

FIG. 5

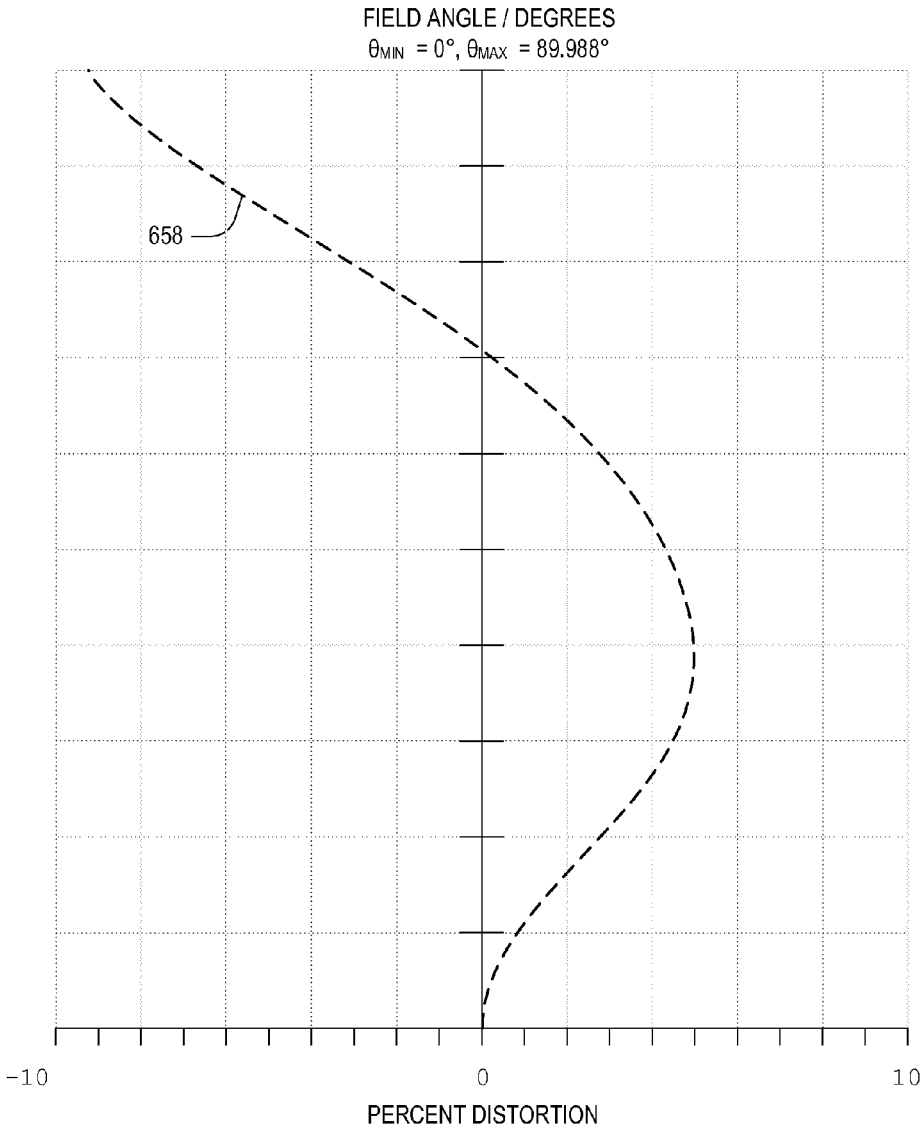
FIELD ANGLE / DEGREES
θMIN = 0°, θMAX = 89.988°
658
-10
0
10
PERCENT DISTORTION

FIG. 6

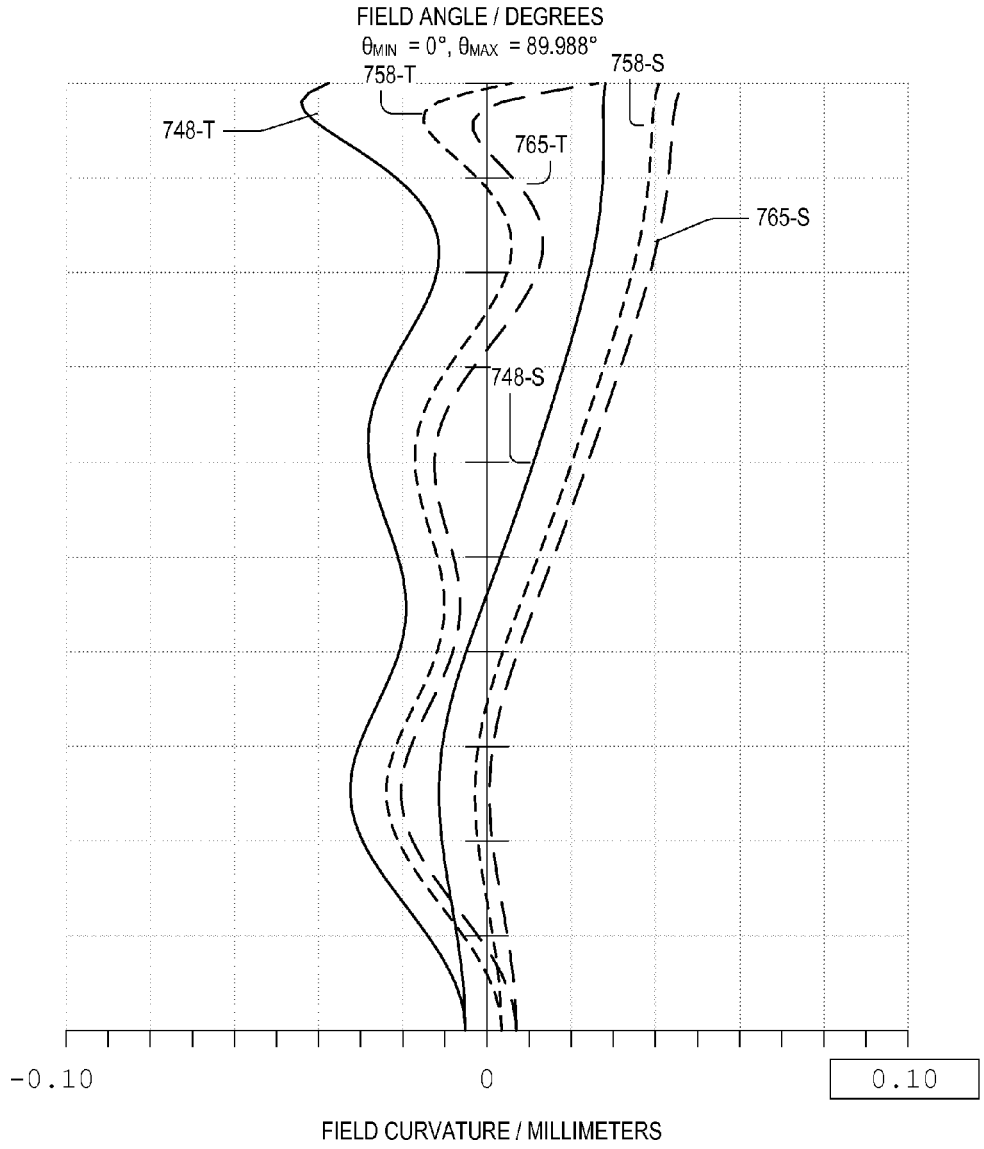
FIELD ANGLE / DEGREES
θMIN = 0°, θMAX = 89.988°
758-T
758-S
748-T
765-T
765-S
748-S
-0.10
0
0.10
FIELD CURVATURE / MILLIMETERS

FIG. 7

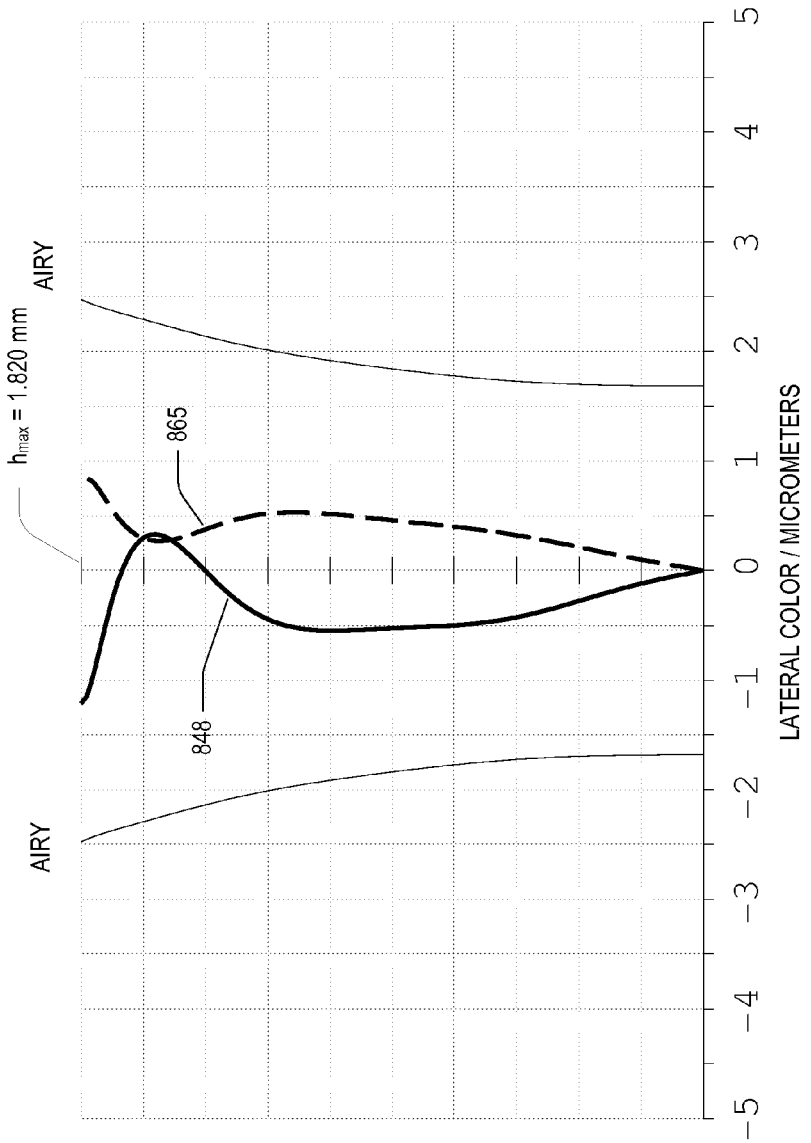
AIRY
AIRY
h_{max} = 1.820 mm
865
848
5
4
3
2
1
0
−1
−2
−3
−4
−5
LATERAL COLOR / MICROMETERS

FIG. 8

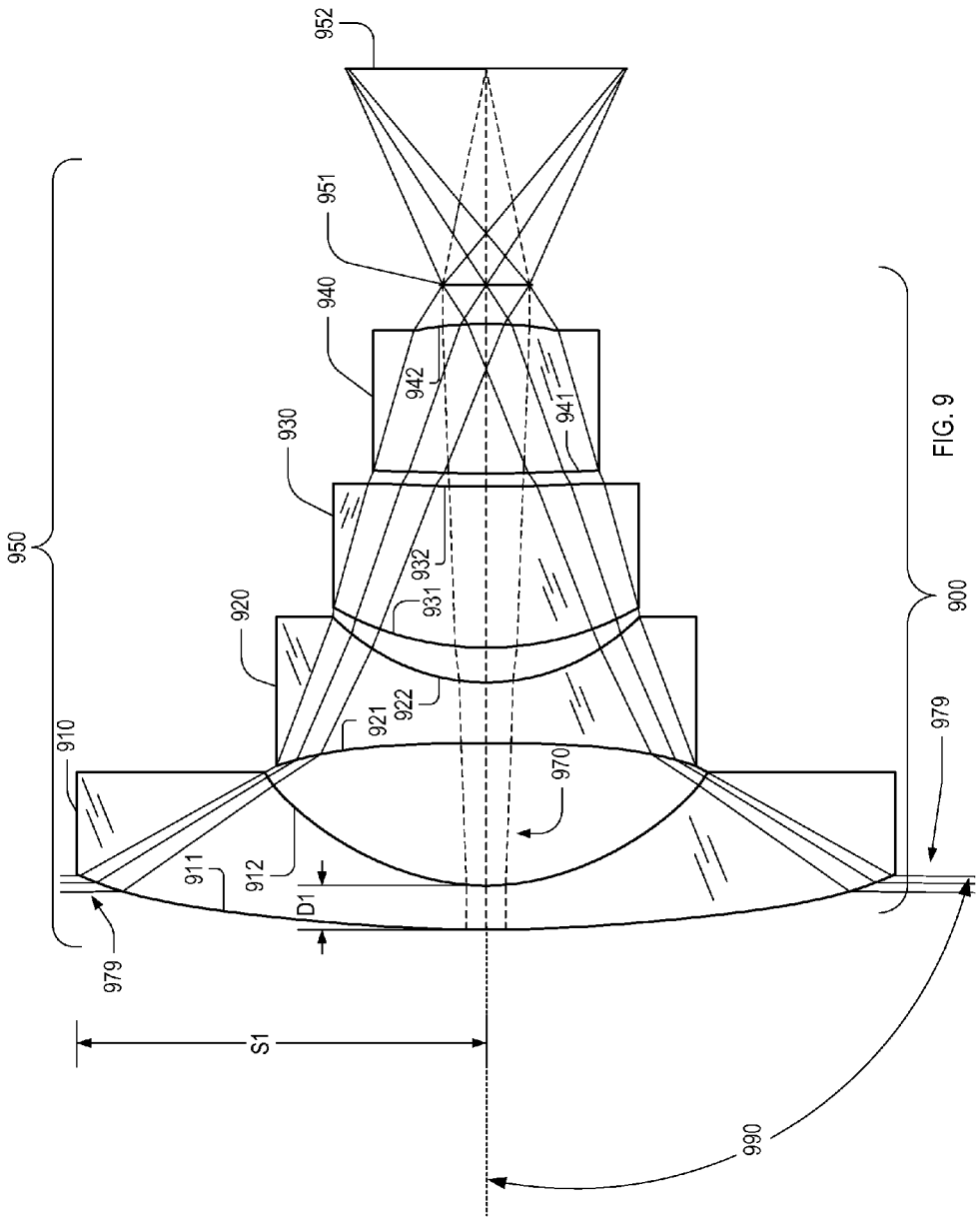
952
951
940
942
941
930
932
931
920
922
921
910
970
911
912
D1
979
979
950
900
S1
990

FIG. 9

1011 surface	1012 radius r_c (mm)	1013 thickness (mm)	1014 n_D (λ=589 nm)	1015 Abbe Number	1016 conic k	aspheric coefficient 1004 4th-order term α_4	1006 6th-order term α_6	1008 8th-order term α_8	1010 10th-order term α_{10}
object	∞	∞	--	--	--	--	--	--	--
911	19.591	0.570	1.543	57	-1.422	-6.8501E-04	2.5042E-05	--	--
912	2.977	1.842			-0.044	-9.5461E-03	9.2518E-04	-1.0111E-04	--
921	-30.653	0.787	1.543	57	20.979	-3.1450E-03	0.0000E+00	--	--
922	2.755	0.449			-0.032	4.6124E-03	-1.0408E-03	--	--
931	4.110	2.083	1.585	30	-1.148	3.0511E-03	1.0880E-04	--	--
932	20.739	0.170			-188.697	-1.3766E-03	--	--	--
941	20.833	1.932	1.523	52	-191.456	-1.9841E-03	2.6812E-04	--	--
942	-5.090	0.500			18.827	6.3574E-03	3.3452E-02	-3.4900E-02	2.5404E-02
951	∞	2.800	(ideal lens)		--	--	--	--	--
952	∞	0.000	--	--	--	--	--	--	--

FIG. 10

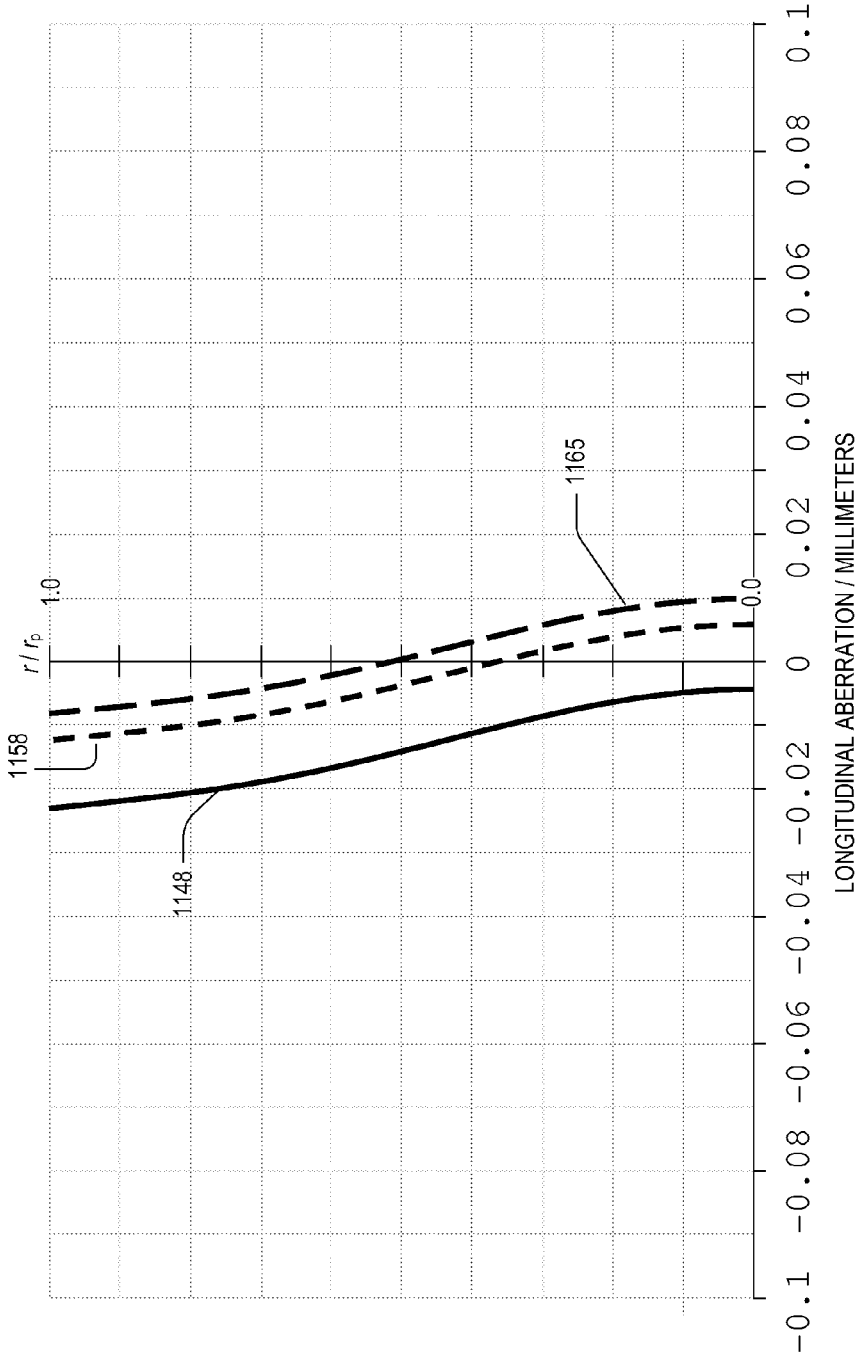
1158
1148
1165
r / r_p
1.0
0.0
0.1
0.08
0.06
0.04
0.02
0
−0.02
−0.04
−0.06
−0.08
−0.1
LONGITUDINAL ABERRATION / MILLIMETERS

FIG. 11

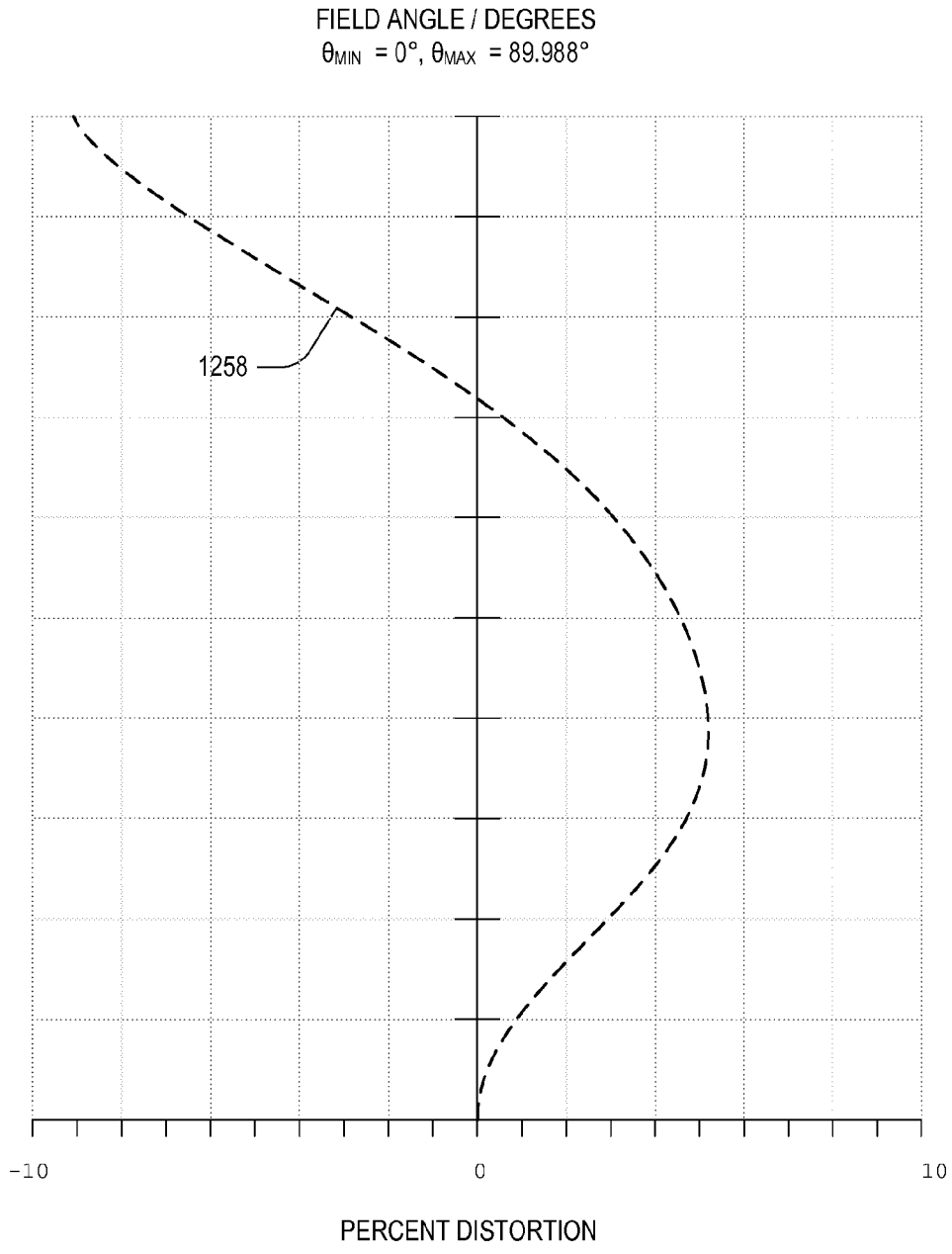
FIELD ANGLE / DEGREES
θMIN = 0°, θMAX = 89.988°
1258
-10
0
10
PERCENT DISTORTION

FIG. 12

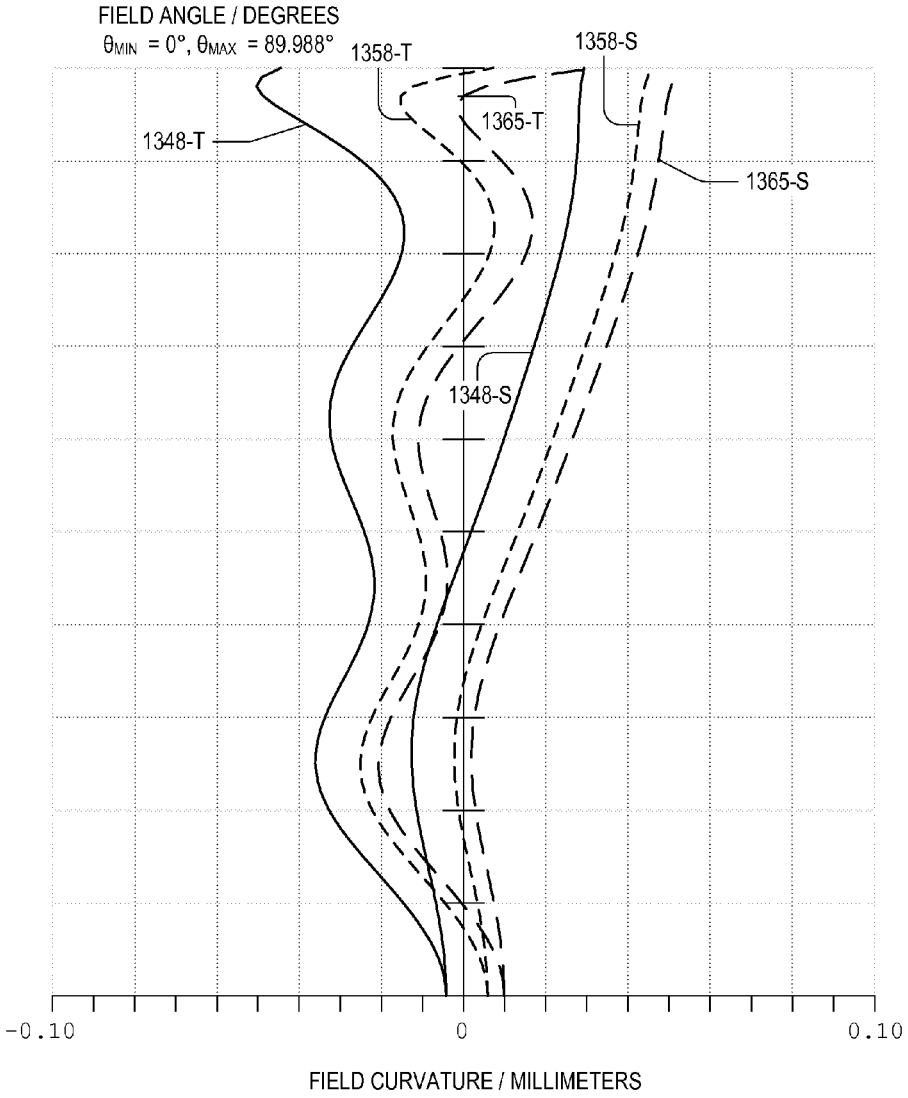
FIELD ANGLE / DEGREES
θMIN = 0°, θMAX = 89.988°
1358-T
1358-S
1365-T
1348-T
1365-S
1348-S
-0.10
0
0.10
FIELD CURVATURE / MILLIMETERS

FIG. 13

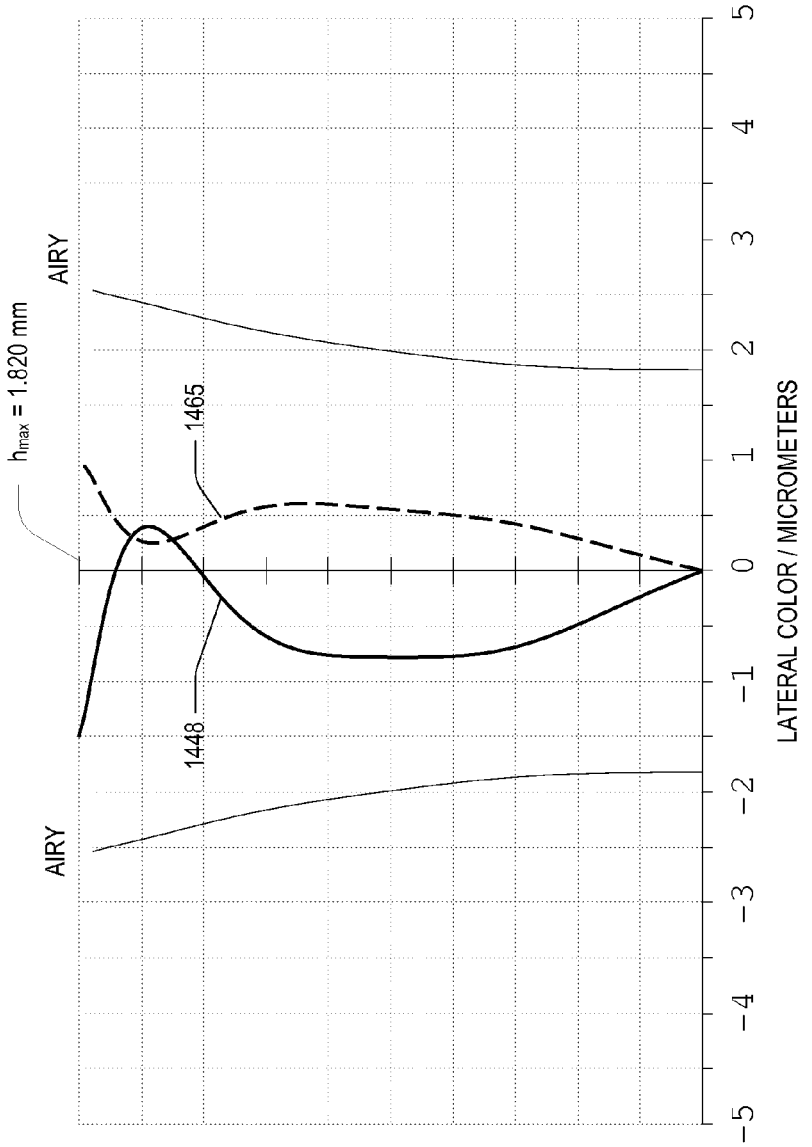
AIRY
h_{max} = 1.820 mm
1465
1448
AIRY
5
4
3
2
1
0
−1
−2
−3
−4
−5
LATERAL COLOR / MICROMETERS

FIG. 14

FOUR-PIECE ALL-ASPHERIC ADAPTER FISHEYE LENS

BACKGROUND

Digital camera modules are used in a variety of consumer, industrial and scientific imaging devices to produce still images and/or video. These devices include mobile telephones, digital still image and video cameras, and webcams. The field of view of a camera module is typically between 60 degrees and 70 degrees. The field of view can be increased by attaching an adapter lens in front of the camera module. The resulting imaging system of the adapter lens and camera module has a wider field of view than the camera module alone. A wide field of view is valuable in applications such as autonomous vehicle navigation, car parking monitor systems, and gesture recognition.

SUMMARY OF THE INVENTION

According to an embodiment, a four-piece all-aspheric adapter fisheye (FPAAAF) lens is provided. The FPAAAF lens includes a negative meniscus lens, a biconcave lens, a positive meniscus lens, and a biconvex lens. The biconcave lens is between the negative meniscus lens and the positive meniscus lens; the positive meniscus lens is between the biconcave lens and the biconvex lens. The negative meniscus lens, the biconcave lens, the positive meniscus lens, and the biconvex lens are coaxial and arranged with an exit pupil to cooperatively generate an image with a camera lens that has greater field of view than the camera lens alone when the exit pupil is coplanar and coaxial with an entrance pupil of the camera lens. Each of the negative meniscus lens, the biconcave lens, the positive meniscus lens, and the biconvex lens has an aspheric object-side surface and an aspheric image-side surface;

According to an embodiment, the negative meniscus lens has a thickness D**1** and the object-side surface with a semi-diameter S**1**, wherein ratio S**1**/D**1** satisfies 9.0<S**1**/D**1**<9.8 for enabling a wide field of view. The negative meniscus lens has a focal length F**1** and the object-side surface having a radius of curvature R**1**, wherein ratio F**1**/R**1** satisfies −0.4<F**1**/R**1**<−0.3 for reducing distortion. The object-side surface of the biconcave lens has a radius of curvature R**3**; the image-side surface of the biconcave lens has a radius of curvature R**4**, wherein ratio R**4**/R**3** satisfies −0.12<R**4**/R**3**<−0.04 for reducing field curvature. The object-side surface of the positive meniscus lens has a positive radius of curvature R**5** and the image-side surface of the positive meniscus lens has a positive radius of curvature R**6**, wherein R**6** exceeds R**5** for reducing chromatic aberration. The object-side surface of the biconvex lens has a radius of curvature R**7** and the image-side surface of the biconvex lens has a radius of curvature R**8**, wherein ratio R**8**/R**7** satisfies −0.28<R**8**/R**7**<−0.2 for reducing longitudinal aberration. The negative meniscus lens and biconcave lens each have an Abbe number exceeding 55, and the positive meniscus lens has an Abbe number less than 35, for reducing chromatic aberration.

BRIEF DESCRIPTION OF THE FIGURES

FIG. **1** shows a prior art adapter fisheye lens within an adapter housing that is attached to a mobile phone.

FIG. **2** is a cross-sectional view of a four-piece all-aspheric adapter fisheye (FPAAAF) lens, in an embodiment.

FIG. **3** is a cross-sectional view of a FPAAAF lens functioning as an adapter lens for an imaging system, in an embodiment.

FIG. **4** shows exemplary parameters for the FPAAAF lens of FIG. **3**.

FIG. **5** is a plot of the longitudinal aberration of the FPAAAF lens within the imaging system of FIG. **3**.

FIG. **6** is a plot of the f-Theta distortion of the FPAAAF lens within the imaging system of FIG. **3**.

FIG. **7** is a plot of the Petzval field curvature of the FPAAAF lens within the imaging system of FIG. **3**.

FIG. **8** is a plot of the lateral color error of the FPAAAF lens within the imaging system of FIG. **3**.

FIG. **9** is a cross-sectional view of a FPAAAF lens functioning as an adapter lens for an imaging system, in an embodiment.

FIG. **10** shows exemplary parameters for the fisheye lens of FIG. **9**.

FIG. **11** is a plot of the longitudinal aberration of the FPAAAF lens within the imaging system of FIG. **9**.

FIG. **12** is a plot of the f-Theta distortion of the FPAAAF lens within the imaging system of FIG. **9**.

FIG. **13** is a plot of the Petzval field curvature of the FPAAAF lens within the imaging system of FIG. **9**.

FIG. **14** is a plot of the lateral color error of the FPAAAF lens within the imaging system of FIG. **9**.

DETAILED DESCRIPTION

FIG. **1** shows a prior-art adapter fisheye lens **100** within a fisheye lens adapter housing **140** that is attached to a mobile phone **150**. Mobile phone **150** includes an on-chip camera with a standard field of view. Fisheye lens adapter housing **140** is positioned on mobile phone **150** such that the optic axis of adapter fisheye lens **100** and the optic axis of the on-chip phone camera are coaxial.

Prior-art adapter fisheye lens **100** includes optical elements made of optical glass and/or plastic, for example, one spherical glass lens combined with one aspherical plastic lens. The range of Abbe numbers V_D of optical glasses exceeds that of optical plastics. Thus, the minimum chromatic aberration achievable in compound fisheye lenses with only spherical glass surfaces is lower than a similar lens formed from plastic. However, compared to an all-plastic lens system, the use of a glass in a fisheye lens incurs increased material costs, fabrication costs, weight, volume, and restrictions on manufacturing lens shape.

An all-plastic compound fisheye lens described hereinbelow achieves the performance benefits of glass with the size and weight advantages of plastic. Using aspherical surfaces, rather than just spherical surfaces, more degrees of freedom are achieved when optimizing an all-plastic fisheye lens design to meet desired performance specifications. These performance specifications include minimizing aberrations such as longitudinal aberration (longitudinal spherical aberration), image distortion, field curvature, and lateral color. Optimizing a lens design per these performance metrics is constrained by the relatively narrow range of Abbe numbers in optical plastics, and the benefits of minimizing the number of plastic elements.

This disclosure specifically provides four-piece all-aspheric adapter fisheye (FPAAAF) lenses, wherein the Abbe numbers of each optical element in the FPAAAF corresponds to an existing optical plastic. The FPAAAF lens may be designed to fit into fisheye lens adapter housings, such as fisheye lens adapter housing **140** of FIG. **1**.

FIG. **2** is a cross-sectional view of one FPAAAF lens **200**. FPAAAF lens **200** includes a negative meniscus lens **210**, a biconcave lens **220**, positive meniscus lens **230**, and a biconvex lens **240**. Negative meniscus lens **210** includes an object-side surface **211** and an image-side surface **212**. Biconcave lens **220** includes an object-side surface **221** and an image-side surface **222**. Positive meniscus lens **230** includes an object-side surface **231** and an image-side surface **232**. Biconvex lens **240** includes an object-side surface **241** and an image-side surface **242**. In a first embodiment of FPAAAF lens **200**, each of the surfaces **211**, **212**, **221**, **222**, **231**, **232**, **241**, and **242** are aspheric.

Negative meniscus lens **210**, biconcave lens **220**, positive meniscus lens **230**, and biconvex lens **240** are each singlet lenses. In an embodiment of FPAAAF lens **200**, one or more of negative meniscus lens **210**, biconcave lens **220**, positive meniscus lens **230**, and biconvex lens **240** may be non-singlet lenses without departing from the scope hereof. FPAAAF lens **200** may be dimensioned so that it replaces adapter fisheye lens **100** in fisheye lens adapter housing **140**, FIG. **1**.

Referring to negative meniscus lens **210**, the semi-diameter of object-side surface **211** is S**1** and the on-axis thickness of negative meniscus lens **210** is D**1**. Embodiments of negative meniscus lens **210** may have a quotient S**1**/D**1** between 9.0 and 9.8. Limiting the quotient S**1**/D**1** to this range enables a wide field of view in imaging systems that include FPAAAF lens **200**. For example, imaging systems **350** and **950** discussed herein have respective fields of view exceeding 170°.

Negative meniscus lens **210** has a focal length F**1** and a radius of curvature R**1** of object-side surface **211**. Embodiments of negative meniscus lens **210** may have a quotient F**1**/R**1** between −0.4 and −0.3. Limiting the quotient F**1**/R**1** to this range allows for correcting distortion in imaging systems that include FPAAAF lens **200**. For example, at field angles between 0° and 90°, imaging systems **350** and **950** discussed herein have respective distortions less than 10%.

Referring to biconcave lens **220**, object-side surface **221** has radius of curvature R**3** and image-side surface **222** has radius of curvature R**4**. Embodiments of biconcave lens **220** may have a quotient R**4**/R**3** between −0.12 and −0.04. Limiting the quotient R**4**/R**3** to this range allows for correcting field curvature in imaging systems that include FPAAAF lens **200**. For example, at field angles between 0° and 90°, imaging systems **350** and **950** discussed herein have respective field curvatures less than 0.06 mm.

Referring to positive meniscus lens **230**, object-side surface **231** has radius of curvature R**5** and image-side surface **232** has radius of curvature R**6**. In embodiments of positive meniscus lens **230**, R**6**>R**5**>0, which ensures that lens **230** is a positive lens. Requiring R**6**>R**5**>0 allows for reducing chromatic aberration in imaging systems that include FPAAAF lens **200**, such as imaging systems **350** and **950** discussed herein. For example, the transverse chromatic aberration (lateral color error) of imaging systems **350** and **950** discussed herein is less than the Airy disk radius.

Referring to biconvex lens **240**, object-side surface **241** has radius of curvature R**7** and image-side surface **242** has radius of curvature R**8**. Embodiments of biconvex lens **240** may have a quotient R**8**/R**7** between −0.28 and −0.20. Limiting the quotient R**7**/R**8** to this range allows for correcting longitudinal aberration in imaging systems that include FPAAAF lens **200**, such as imaging systems **350** and **950** discussed herein.

In FPAAAF lens **200**, negative meniscus lens **210** and biconcave lens **220** each have Abbe number V_D>55. Positive meniscus lens **230** has an Abbe number V_D<35. These constraints on Abbe numbers allow for correcting chromatic aberration in imaging systems that include FPAAAF lens **200**, such as imaging systems **350** and **950** discussed herein.

The *Handbook of Plastic Optics* (Wiley-VCH, publisher) lists examples of transparent optical materials with V_D>55. These include polymethyl methacrylate (PMMA), and cycloolefin polymers, for example, APEL™ 5014DP, TOPAS® 5013, and ZEONEX® 480R. The lens material with V_D>55 may be plastic, glass, or any non-plastic optical material without departing from the scope hereof.

The *Handbook of Plastic Optics* lists examples of transparent optical materials with V_D<35. These include PANLITE®, a brand-name polycarbonate, Udel® P-1700, a brand-name polysulfone, and OKP-4, a brand-name optical polyester. The lens material with V_D<35 may be plastic, glass, or any non-plastic optical material without departing from the scope hereof.

Lenses **210**, **220**, **230**, and **240** may be formed by injection molding or other methods known in the art. Embodiments of lenses **210**, **220**, **230**, and **240** formed of glass may be formed by precision glass molding (also known as ultra-precision glass pressing) or other methods known in the art.

FPAAAF Lens

Example 1

FIG. **3** is a cross-sectional view of a FPAAAF lens **300** functioning as an adapter lens for an imaging system, e.g., for a standard non-fisheye imaging system included in mobile phone **150**, FIG. **1**. FPAAAF lens **300** is an embodiment of FPAAAF lens **200**. FPAAAF lens **300** includes a negative meniscus lens **310**, a biconcave lens **320**, a positive meniscus lens **330**, and a biconvex lens **340** that are analogous to negative meniscus lens **210**, biconcave lens **220**, positive meniscus lens **230**, and biconvex lens **240** of FPAAAF lens **200**. Negative meniscus lens **310** includes an object-side surface **311** and an image-side surface **312**. Biconcave lens **320** includes an object-side surface **321** and an image-side surface **322**. Positive meniscus lens **330** includes an object-side surface **331** and an image-side surface **332**. Biconvex lens **340** includes an object-side surface **341** and an image-side surface **342**. In FPAAAF lens **300**, each of the surfaces **311**, **312**, **321**, **322**, **331**, and **332** are aspheric.

Specifically, FPAAAF lens **300** is shown coupled with a camera lens **351** of the standard non-fisheye imaging system such that, collectively, FPAAAF lens **300** and camera lens **351** cooperatively form an image at image plane **352**.

FPAAAF lens **300** is variably locatable with respect to a camera lens **351**. In FIG. **3**, the entrance pupil of camera lens **351** is located at the exit pupil of FPAAAF lens **300**, resulting in an imaging system **350**. In imaging system **350**, the entrance pupil of camera lens **351** and the exit pupil of FPAAAF lens **300** are coaxial and coplanar.

Camera lens **351** is, for example, an imaging lens of a reflowable camera module mounted on a printed circuit board (PCB) of an imaging device such as a mobile phone. But camera lens **351** may alternatively be an imaging lens of other cameras known in the art without departing from the scope hereof; examples include point-and-shoot cameras, compact system cameras, and single-lens reflex cameras. Such cameras may capture still images, video, or both, and be either digital or analog.

For the purpose of characterizing the aberrations caused by FPAAAF lens **300**, camera lens **351** is modeled as an aberration-free "perfect lens" with a 66° field of view. However, camera lens **351** may include aberrations and have a different field of view without departing from the scope hereof.

Imaging system **350** is shown with ray traces of ray pencils **370** and **379** computed and displayed by the Zemax® Optical Design Program. Ray pencil **370** and ray pencil **379** propagate from the center and edge of the scene, respectively, through FPAAAF lens **300** and camera lens **351**, and focus at image plane **352**. Ray pencil **370** has a ray angle of zero. Ray pencil **379** has a ray angle **390** equal to 90°. Being axially symmetric, imaging system **350** has a field of view that is twice ray angle **390**, or 180°.

FIG. **4** shows exemplary parameters of each surface of FPAAAF lens **300**. Surface column **411** denotes surfaces **311**, **312**, **321**, **322**, **331**, **332**, **341**, **342**, camera lens **351**, and image plane **352** shown in FIG. **3**. Column **414** lists the material's refractive index n_D at λ=589.3 nm, and column **415** lists the corresponding Abbe numbers V_D. Negative meniscus lens **310** has refractive index n_D=1.543, Abbe number V_D=57, and includes object-side surface **311** and image-side surface **312**. Biconcave lens **320** has refractive index n_D=1.543, Abbe number V_D=57, and includes object-side surface **321** and image-side surface **322**. Positive meniscus lens **330** has refractive index n_D=1.632, Abbe number V_D=23, and includes object-side surface **331** and image-side surface **332**. Biconvex lens **340** has refractive index n_D=1.510, Abbe number V_D=57, and includes object-side surface **341** and image-side surface **342**.

In FPAAAF lens **300**, negative meniscus lens **310**, biconcave lens **320**, and biconvex lens **340** each have Abbe number V_D=57. This satisfies a condition that three—and only three—of the three lenses of FPAAAF lens **300** have an Abbe number V_D>55. The third lens in FPAAAF lens **300**, positive meniscus lens **330**, has Abbe number V_D=23, which satisfies a condition that one—and only one—of the three lenses of FPAAAF lens **300** has an Abbe number V_D<35.

Column **413** includes on-axis thickness values, in millimeters, between surfaces **311**, **312**, **321**, **322**, **331**, **332**, **341** and **342**. Surfaces **311**, **312**, **321**, **322**, **331**, **332**, **341** and **342** are defined by surface sag z_{sag}, Eqn. 1.

$$z_{sag} = \frac{cr^2}{1+\sqrt{1-(1+k)c^2r^2}} + \sum_{i=1}^{N} \alpha_i r^i \quad (1)$$

In Eqn. 1, z_{sag} is a function of radial coordinate r, where directions z and r are shown in coordinate axes **398**, FIG. **3**. In Eqn. 1, the parameter c is the reciprocal of the surface radius of curvature r_c: $c=1/r_c$. Column **412** of FIG. **4** lists r_c values for surfaces **311**, **312**, **321**, **322**, **331**, **332**, **341**, and **342**. Parameter k denotes the conic constant, shown in column **416**. Columns **404**, **406**, **408**, and **410** contain values of aspheric coefficients α_4, α_6, α_8, and α_{10}, respectively. The units of quantities in FIG. **3** are consistent with z_{sag} in Eqn. 1 being expressed in millimeters.

Referring to negative meniscus lens **310**, FIG. **3**, the semi-diameter of object-side surface **311** is S**1** and the on-axis thickness of negative meniscus lens **310** is D**1**. The ratio S**1**/D**1**=9.7. Negative meniscus lens **310** has a focal length F**1**=−6.711 mm. Object-side surface **311** has radius of curvature R**1**=21.071 mm. The ratio F**1**/R**1**=−0.319.

Referring to biconcave lens **320**, FIG. **3**, object-side surface **321** has radius of curvature R**3**=−41.543 mm and image-side surface **322** has radius of curvature R**4**=3.126 mm. The ratio R**4**/R**3**=−0.0752.

Referring to positive meniscus lens **330**, FIG. **3**, object-side surface **331** has radius of curvature R**5**=5.386 and image-side surface **332** has radius of curvature R**6** that exceeds R**5** (R**6**=16.782).

Referring to biconvex lens **340**, FIG. **3**, object-side surface **341** has radius of curvature R**7**=20.303 and image-side surface **342** has radius of curvature R**8**=−4.746. The ratio R**8**/R**7**=−0.2338.

FIGS. **5-8** are plots of longitudinal aberration, f-Theta distortion, field curvature, and lateral color, respectively, of FPAAAF lens **300** within imaging system **350** as computed by Zemax®. Since camera lens **351** does not contribute to the aberrations shown in FIG. **5-8**, the FPAAAF lens **300** is the source of these aberrations. The Zemax® User's Manual includes detailed definitions of each of these quantities.

FIG. **5** is a plot of the longitudinal aberration of FPAAAF lens **300** within imaging system **350**. In FIG. **5**, longitudinal aberration is plotted in units of millimeters as a function of normalized radial coordinate r/r_p, where r_p=0.2793 mm is the maximum entrance pupil radius. Longitudinal aberration curves **548**, **558**, and **565** are computed at the blue, green, and red Fraunhofer F-, D- and C-spectral lines: λ_F=486.1 nm, λ_D=589.3 nm, and λ_C=656.3 nm respectively.

FIG. **6** is a plot of the f-Theta distortion, versus field angle, of FPAAAF lens **300** within imaging system **350**. The maximum field angle plotted in FIG. **6** is θ_{max}=89.998°. Distortion curve **658** is computed at wavelength λ_D. For clarity, distortion curves corresponding to wavelength λ_F and λ_C are not shown, as they overlap distortion curve **658** to within its line thickness as plotted in FIG. **6**.

FIG. **7** is a plot of the Petzval field curvature of TPAAAF lens **300** as a function of field angle of FPAAAF lens **300** within imaging system **350**. The field curvature is plotted for field angles between zero and is θ_{max}=89.998°. Field curvature **748**-S and field curvature **748**-T (solid lines) are computed at wavelength λ_F in the sagittal and tangential planes, respectively. Field curvature **758**-S and field curvature **758**-T (short-dashed lines) are computed at wavelength λ_D in the sagittal and tangential planes, respectively. Field curvature **765**-S and field curvature **765**-T (long-dashed lines) correspond to field curvature at wavelength λ_C in the sagittal and tangential planes, respectively.

FIG. **8** is a plot of the lateral color error, also known as transverse chromatic aberration, versus field height of FPAAAF lens **300** within imaging system **350**. Field height ranges from h_{min}=0 (on-axis) to h_{max}=1.820 mm in image plane **352**. Lateral color is referenced to λ_D: the lateral color for λ_D is zero for all field heights. Lateral color **848** is computed at wavelength λ_F. Lateral color **865** is computed at wavelength λ_C. The lateral color error is less than the Airy disk radius for the range of field heights evaluated.

FPAAAF Lens

Example 2

FIG. **9** is a cross-sectional view of a FPAAAF lens **900** functioning as an adapter lens for an imaging system, e.g., for a standard non-fisheye imaging system included in mobile phone **150**, FIG. **1**. FPAAAF lens **900** is an embodiment of FPAAAF lens **200**. FPAAAF lens **900** includes a negative meniscus lens **910**, a biconcave lens **920**, a positive meniscus lens **930**, and a biconvex lens **940** that are analogous to negative meniscus lens **210**, biconcave lens **220**, positive meniscus lens **230**, and biconvex lens **240** of FPAAAF lens **200**. Negative meniscus lens **910** includes an object-side surface **911** and an image-side surface **912**. Biconcave lens **920** includes an object-side surface **921** and an image-side surface **922**. Positive meniscus lens **930** includes an object-side surface **931** and an image-side surface **932**. Biconvex lens **940** includes an object-side surface **941** and an image-side surface

942. In FPAAAF lens 900, each of the surfaces 911, 912, 921, 922, 931, 932, 941, and 942 are aspheric.

Specifically, FPAAAF lens 900 is shown coupled with a camera lens 951 of the standard non-fisheye imaging system such that, collectively, FPAAAF lens 900 and camera lens 951 cooperatively form an image at image plane 952.

FPAAAF lens 900 is variably locatable with respect to a camera lens 951. In FIG. 9, the entrance pupil of camera lens 951 is located at the exit pupil of FPAAAF lens 900, resulting in an imaging system 950. In imaging system 950, the entrance pupil of camera lens 951 and the exit pupil of FPAAAF lens 900 are coaxial and coplanar.

Camera lens 951 is, for example, an imaging lens of a reflowable camera module mounted on a PCB of an imaging device. For the purpose of characterizing the aberrations caused by FPAAAF lens 900, in FIG. 9 camera lens 951 is modeled as an aberration-free "perfect lens" with a 66° field of view. Camera lens 951 is similar to camera lens 351.

Imaging system 950 is shown with ray traces of ray pencils 970 and 979 computed and displayed by the Zemax® Optical Design Program. Ray pencil 970 and ray pencil 979 propagate from the center and edge of the scene, respectively, through FPAAAF lens 900 and camera lens 951, and focus at image plane 952. Ray pencil 970 has a ray angle of zero. Ray pencil 979 has a ray angle 990 equal to 90°. Being axially symmetric, imaging system 950 has a field of view that is twice ray angle 990, or 180°.

FIG. 10 shows parameters of each surface of FPAAAF lens 900. Surface column 1011 denotes surfaces 911, 912, 921, 922, 931, 932, 941, 942, camera lens 951, and image plane 952 shown in FIG. 9. Meniscus lens 910 has refractive index n_D=1.543, Abbe number V_D=57, and includes surface 911 and surface 912. Biconcave lens 920 has refractive index n_D=1.543, Abbe number V_D=57, and includes surface 921 and surface 922. Positive meniscus lens 930 has refractive index n_D=1.585, Abbe number V_D=30, and includes object-side surface 931 and image-side surface 932. Biconvex lens 940 has refractive index n_D=1.523, Abbe number V_D=52, and includes object-side surface 941 and image-side surface 942.

Column 1013 contains thickness values, in millimeters, between surfaces 911, 912, 921, 922, 931, 932, 941, and 942. Surfaces 911, 912, 921, 922, 931, and 932 are defined by z_{sag}, Eqn. 1. Columns 1012, 1014, 1015, 1016, 1004, 1006, 1008, and 1010 are similar to columns 412, 414, 415, 416, 404, 406, 408, and 410, respectively, of FIG. 4.

Referring to meniscus lens 910, FIG. 9, the semi-diameter of the object side of meniscus lens 910 is S1 and the on-axis thickness of meniscus lens 910 is D1. The ratio S1/D1=9.7.

Meniscus lens 910 is a negative lens with a focal length F1=−6.544 mm. Object-side surface 911 has radius of curvature R1=19.591. The ratio F1/R1=−0.334.

Referring to biconcave lens 920, FIG. 9, object-side surface 921 has radius of curvature R3=−30.653 mm and image-side surface 922 has radius of curvature R4=2.755 mm. The ratio R4/R3=−0.0899.

Referring to positive meniscus lens 930, FIG. 9, object-side surface 931 has a radius of curvature R5=4.110, and image-side surface 942 has a radius of curvature R6 the exceeds R5 (R6=20.739).

Referring to biconvex lens 940, FIG. 9, object-side surface 941 has radius of curvature R7=20.833 and image-side surface 942 has radius of curvature R8=−5.090. The ratio R8/R7=−0.2443.

FIGS. 11-14 are plots of longitudinal aberration, f-Theta distortion, field curvature, and lateral color, respectively, of FPAAAF lens 900 within imaging system 950 as computed by Zemax®. Since camera lens 951 does not contribute to the aberrations shown in FIG. 11-14, the FPAAAF lens 900 is the source of these aberrations.

FIG. 11 is a plot of the longitudinal aberration of FPAAAF lens 900 within imaging system 950. In FIG. 11, longitudinal aberration is plotted in units of millimeters as a function of normalized radial coordinate r/r_p, where r_p=0.2793 mm is the maximum entrance pupil radius. Longitudinal aberration curves 1148, 1158, and 1165 are computed at λ_F, λ_D, and λ_C respectively.

FIG. 12 is a plot of the f-Theta distortion, versus field angle, of FPAAAF lens 900 within imaging system 950. The f-Theta distortion is plotted for field angles between zero and is θ_{max}=89.998°. Distortion curve 1258 is computed at wavelength λ_D. For clarity, distortion curves corresponding to wavelength λ_F and λ_C are not shown, as they overlap distortion curve 1258 to within its line thickness as plotted in FIG. 12.

FIG. 13 is a plot of the Petzval field curvature as a function of field angle of FPAAAF lens 900 within imaging system 950. The field curvature is plotted for field angles between zero and is θ_{max}=89.998°. Field curvature curves 1348-S and 1348-T (solid lines) are computed at wavelength λ_F in the sagittal and tangential planes, respectively. Field curvature curves 1358-S and 1358-T (short-dashed lines) are computed at wavelength λ_D in the sagittal and tangential planes, respectively. Field curvature curves 1365-S and 1365-T (long-dashed lines) correspond to field curvature at wavelength λ_C in the sagittal and tangential planes, respectively.

FIG. 14 is a plot of the lateral color error versus field height of FPAAAF lens 900 within imaging system 950. Field height ranges from h_{min}=0 (on-axis) to h_{max}=1.820 mm in image plane 952. Lateral color is referenced to λ_D: the lateral color for λ_D is zero for all field heights. Lateral color 1448 is computed at wavelength λ_F. Lateral color 1465 is computed at wavelength λ_C. Lateral color 1448 and lateral color 1465 are each less than the Airy disk radius for the full range of field heights evaluated.

Combinations of Features

Features described above as well as those claimed below may be combined in various ways without departing from the scope hereof. For example, it will be appreciated that aspects of FPAAAF lens described herein may incorporate or swap features of another FPAAAF lens described herein. The following examples illustrate possible, non-limiting combinations of embodiments described above. It should be clear that many other changes and modifications may be made to the methods and device herein without departing from the spirit and scope of this invention:

(A1) A four-piece all-aspheric adapter fisheye (FPAAAF) lens, the FPAAAF lens comprising a negative meniscus lens, a biconcave lens, a positive meniscus lens, and a biconvex lens. The biconcave lens is between the negative meniscus lens and the positive meniscus lens; the positive meniscus lens is between the biconcave lens and the biconvex lens. The negative meniscus lens, the biconcave lens, the positive meniscus lens, and the biconvex lens are coaxial and arranged with an exit pupil to cooperatively generate an image with a camera lens that has greater field of view than the camera lens alone when the exit pupil is coplanar and coaxial with an entrance pupil of the camera lens. Each of the negative meniscus lens, the biconcave lens, the positive meniscus lens, and the biconvex lens has an aspheric object-side surface and an aspheric image-side surface.

(A2) In the FPAAAF lens denoted as (A1), each of the negative meniscus lens, the biconcave lens, the positive meniscus lens, and the biconvex lens is a singlet lens.

(A3) In either of the FPAAAF lenses denoted as (A1) or (A2), the camera lens has a first field of view less than 90 degrees; the negative meniscus lens, biconcave lens, positive meniscus lens, biconvex lens, and the camera lens cooperatively have a second field of view exceeding 170 degrees.

(A4) In any of the FPAAAF lenses denoted as (A1) through (A3), each of the negative meniscus lens, the biconcave lens, the positive meniscus lens, and the biconvex lens is formed of a plastic material.

(A5) In any of the FPAAAF lenses denoted as (A1) through (A4), each of the negative meniscus lens, the biconcave lens, the positive meniscus lens, and the biconvex lens is injection molded.

(A6) In any of the FPAAAF lenses denoted as (A1) through (A5), the negative meniscus lens has a thickness D**1** and the object-side surface has a semi-diameter S**1**, wherein ratio S**1**/D**1** satisfies 9.0<S**1**/D**1**<9.8.

(A7) In any of the FPAAAF lenses denoted as (A1) through (A6), the negative meniscus lens has a focal length F**1** and the object-side surface has a radius of curvature R**1**; wherein ratio F**1**/R**1** satisfies −0.4<F**1**/R**1**<−0.3.

(A8) In any of the FPAAAF lenses denoted as (A1) through (A7), the object-side surface of the biconcave lens has a radius of curvature R**3**; the image-side surface of the biconcave lens has a radius of curvature R**4**; wherein ratio R**4**/R**3** satisfies −0.12<R**4**/R**3**<−0.04.

(A9) In any of the FPAAAF lenses denoted as (A1) through (A8), the object-side surface of the positive meniscus lens has a positive radius of curvature R**5**; the image-side surface of the positive meniscus lens has a positive radius of curvature R**6**, wherein R**6** exceeds R**5**.

(A10) In any of the FPAAAF lenses denoted as (A1) through (A9), the object-side surface of the biconvex lens has a radius of curvature R**7**; the image-side surface of the biconvex lens has a radius of curvature R**8**; wherein ratio R**8**/R**7** satisfies −0.28<R**8**/R**7**<−0.20.

(A11) In any of the FPAAAF lenses denoted as (A1) through (A10), the negative meniscus lens and biconcave lens each have an Abbe number exceeding 55, and the positive meniscus lens has an Abbe number less than 35, for reducing chromatic aberration. Changes may be made in the above methods and systems without departing from the scope hereof. It should thus be noted that the matter contained in the above description or shown in the accompanying drawings should be interpreted as illustrative and not in a limiting sense. The following claims are intended to cover all generic and specific features described herein, as well as all statements of the scope of the present method and system, which, as a matter of language, might be said to fall there between.

What is claimed is:

1. A four-piece all-aspheric adapter fisheye (FPAAAF) lens, comprising:

a negative meniscus lens, a biconcave lens, a positive meniscus lens, and a biconvex lens;

the biconcave lens being between the negative meniscus lens and the positive meniscus lens; the positive meniscus lens being between the biconcave lens and the biconvex lens;

the negative meniscus lens, the biconcave lens, the positive meniscus lens, and the biconvex lens being coaxial and arranged with an exit pupil to cooperatively generate an image with a camera lens that has greater field of view than the camera lens alone when the exit pupil is coplanar and coaxial with an entrance pupil of the camera lens; and

each of the negative meniscus lens, the biconcave lens, the positive meniscus lens, and the biconvex lens having an aspheric object-side surface and an aspheric image-side surface.

2. The FPAAAF lens of claim **1**, each of the negative meniscus lens, the biconcave lens, the positive meniscus lens, and the biconvex lens being a singlet lens.

3. The FPAAAF lens of claim **1**,

the camera lens having a first field of view less than 90 degrees;

the negative meniscus lens, biconcave lens, positive meniscus lens, biconvex lens, and the camera lens cooperatively having a second field of view exceeding 170 degrees.

4. The FPAAAF lens of claim **1**, each of the negative meniscus lens, the biconcave lens, the positive meniscus lens, and the biconvex lens being formed of a plastic material.

5. The FPAAAF lens of claim **1**, each of the negative meniscus lens, the biconcave lens, the positive meniscus lens, and the biconvex lens being injection molded.

6. The FPAAAF lens of claim **1**, the negative meniscus lens having a thickness D**1** and the object-side surface having a semi-diameter S**1**, wherein ratio S**1**/D**1** satisfies 9.0<S**1**/D**1**<9.8 for enabling a wide field of view.

7. The FPAAAF lens of claim **1**, the negative meniscus lens having a focal length F**1** and the object-side surface having a radius of curvature R**1**; wherein ratio F**1**/R**1** satisfies −0.4<F**1**/R**1**<−0.3 for reducing distortion.

8. The FPAAAF lens of claim **1**, the object-side surface of the biconcave lens having a radius of curvature R**3**; the image-side surface of the biconcave lens having a radius of curvature R**4**; wherein ratio R**4**/R**3** satisfies −0.12<R**4**/R**3**<−0.04 for reducing field curvature.

9. The FPAAAF lens of claim **1**, the object-side surface of the positive meniscus lens having a positive radius of curvature R**5**; the image-side surface of the positive meniscus lens having a positive radius of curvature R**6**, wherein R**6** exceeds R**5** for reducing chromatic aberration.

10. The FPAAAF lens of claim **1**, the object-side surface of the biconvex lens having a radius of curvature R**7**; the image-side surface of the biconvex lens having a radius of curvature R**8**; wherein ratio R**8**/R**7** satisfies −0.28<R**8**/R**7**<−0.20 for reducing longitudinal aberration.

11. The FPAAAF lens of claim **1**, the negative meniscus lens and biconcave lens each having an Abbe number exceeding 55, and the positive meniscus lens having an Abbe number less than 35, for reducing chromatic aberration.

12. A four-piece all-aspheric adapter fisheye (FPAAAF) lens, comprising:

a negative meniscus lens, a biconcave lens, a positive meniscus lens, and a biconvex lens;

the biconcave lens being between the negative meniscus lens and the positive meniscus lens; the positive meniscus lens being between the biconcave lens and the biconvex lens;

the negative meniscus lens, the biconcave lens, the positive meniscus lens, and the biconvex lens being coaxial and arranged with an exit pupil to cooperatively generate an image with a camera lens that has greater field of view than the camera lens alone when the exit pupil is coplanar and coaxial with an entrance pupil of the camera lens;

each of the negative meniscus lens, the biconcave lens, the positive meniscus lens, and the biconvex lens having an aspheric object-side surface and an aspheric image-side surface;

the negative meniscus lens having a thickness D1 and the object-side surface having a semi-diameter S1, wherein ratio S1/D1 satisfies 9.0<S1/D1<9.8 for enabling a wide field of view;

the negative meniscus lens having a focal length F1 and the object-side surface having a radius of curvature R1; wherein ratio F1/R1 satisfies 0.4<F1/R1<0.3 for reducing distortion;

the object-side surface of the biconcave lens having a radius of curvature R3; the image-side surface of the biconcave lens having a radius of curvature R4; wherein ratio R4/R3 satisfies 0.12<R4/R3<0.04 for reducing field curvature;

the object-side surface of the positive meniscus lens having a positive radius of curvature R5; the image-side surface of the positive meniscus lens having a positive radius of curvature R6 exceeds R5 for reducing chromatic aberration;

the object-side surface of the biconvex lens having a radius of curvature R7; the image-side surface of the biconvex lens having a radius of curvature R8; wherein ratio R8/R7 satisfies 0.28<R8/R7<−0.2 for reducing longitudinal aberration; and

the negative meniscus lens and biconcave lens each having an Abbe number exceeding 55, and the positive meniscus lens having an Abbe number less than 35, for reducing chromatic aberration.

13. The FPAAAF lens of claim 12, each of the negative meniscus lens, the biconcave lens, the positive meniscus lens, and the biconvex lens being a singlet lens.

14. The FPAAAF lens of claim 12,

the camera lens having a first field of view less than 90 degrees;

the negative meniscus lens, the biconcave lens, the positive meniscus lens, the biconvex lens, and the camera lens cooperatively having a second field of view exceeding 170 degrees.

15. The FPAAAF lens of claim 12, each of the negative meniscus lens, the biconcave lens, the positive meniscus lens, and the biconvex lens being formed of a plastic material.

16. The FPAAAF lens of claim 12, each of the negative meniscus lens, the biconcave lens, the positive meniscus lens, and the biconvex lens being injection molded.

17. A four-piece all-aspheric adapter fisheye (FPAAAF) lens, comprising:

a negative meniscus lens, a biconcave lens, a positive meniscus lens, and a biconvex lens;

the biconcave lens being between the negative meniscus lens and the positive meniscus lens; the positive meniscus lens being between the biconcave lens and the biconvex lens;

the negative meniscus lens, the biconcave lens, the positive meniscus lens, and the biconvex lens being coaxial and arranged with an exit pupil to cooperatively generate an image with a camera lens that has greater field of view than the camera lens alone when the exit pupil is coplanar and coaxial with an entrance pupil of the camera lens; and

each of the negative meniscus lens, the biconcave lens, the positive meniscus lens, and the biconvex lens having an aspheric object-side surface and an aspheric image-side surface;

the camera lens having a first field of view less than 90 degrees;

the negative meniscus lens, the biconcave lens, the positive meniscus lens, the biconvex lens, and the camera lens cooperatively having a second field of view exceeding 170 degrees;

each of the negative meniscus lens, the biconcave lens, the positive meniscus lens, and the biconvex lens being a singlet lens;

each of the negative meniscus lens, the biconcave lens, the positive meniscus lens, and the biconvex lens being formed of a plastic material;

each of the negative meniscus lens, the biconcave lens, the positive meniscus lens, and the biconvex lens being injection molded;

the negative meniscus lens having a thickness D1 and the object-side surface having a semi-diameter S1, wherein ratio S1/D1 satisfies 9.0<S1/D1<9.8 for enabling a wide field of view;

the negative meniscus lens having a focal length F1 and the object-side surface having a radius of curvature R1; wherein ratio F1/R1 satisfies 0.4<F1/R1<0.3 for reducing distortion;

the object-side surface of the biconcave lens having a radius of curvature R3; the image-side surface of the biconcave lens having a radius of curvature R4; wherein ratio R4/R3 satisfies 0.12<R4/R3<0.04 for reducing field curvature;

the object-side surface of the positive meniscus lens having a positive radius of curvature R5; the image-side surface of the positive meniscus lens having a positive radius of curvature R6 exceeds R5 for reducing chromatic aberration;

the object-side surface of the biconvex lens having a radius of curvature R7; the image-side surface of the biconvex lens having a radius of curvature R8; wherein ratio R8/R7 satisfies 0.28<R8/R7<−0.2 for reducing longitudinal aberration;

the negative meniscus lens and biconcave lens each having an Abbe number exceeding 55, and the positive meniscus lens having an Abbe number less than 35, for reducing chromatic aberration.

* * * * *

UNITED STATES PATENT AND TRADEMARK OFFICE

CERTIFICATE OF CORRECTION

PATENT NO. : 9,304,299 B2
APPLICATION NO. : 14/465146
DATED : April 5, 2016
INVENTOR(S) : Chuen-Yi Yin et al.

It is certified that error appears in the above-identified patent and that said Letters Patent is hereby corrected as shown below:

In The Specification,

Column 1, line 37, "surface;" should read -- surface, --;

In The Claims,

Column 11, line 7, "0.4<F1/R1<0.3" should read -- –0.4 < F1/R1 < –0.3 --;

line 12, "0.12<R4/R3<0.04" should read -- –0.12 < R4/R3 < –0.04 --;

line 22, "0.28 R8/R7<–0.2" should read -- –0.28 < R8/R7 < –0.2 --;

Column 12, line 30, "0.4<F1/R1<0.3" should read -- –0.4 < F1/R1 < –0.3 --;

line 35, "0.12<R4/R3<0.04" should read -- –0.12 < R4/R3 < –0.04 --;

line 45, "0.28<R8/R7<–0.2" should read -- –0.28 < R8/R7 < –0.2 --.

Signed and Sealed this
Fifteenth Day of November, 2016

Michelle K. Lee

Michelle K. Lee
Director of the United States Patent and Trademark Office